



Physical vulnerability evaluation of buildings exposed to Balia Nala landslide using indicator-based approach and GIS: a case study of Nainital town, Uttarakhand, India

Himani Tiwari¹ · Ramesh Veerappan¹ · Harshita Tiwari² · Thomas Oommen³

Received: 24 September 2021 / Accepted: 17 February 2022 / Published online: 18 April 2022
© Saudi Society for Geosciences 2022

Abstract

The Balia Nala landslide in Nainital has become a widely concerning issue due to its frequent reactivation and rampant construction over its slope. It has underscored the importance of characterizing the Balia Nala landslide and quantification of the physical vulnerability of the buildings. The current study incorporates the indicator-based approach with the aid of Geographic Information System (GIS) to assess the site-specific physical vulnerability of the buildings exposed to debris flow landslide. The vulnerability of the 63 household samples was computed using 15 different indicators. Empirical relationships were employed for estimating the intensity of the landslide, resistance of the buildings, physical vulnerability (*PV*), and site-specific vulnerability (*SSV*). A very high landslide intensity of value '1' has been evaluated in the area. 89% and 11% of the surveyed buildings came out to be moderately ($0.5 < R \leq 0.9$) and low resistant ($R \leq 0.5$) respectively. The final study results show that 44% of the surveyed buildings fall under class III ($0.9 < SSV \leq 1$; very severe to complete damage), and about 56% fall under class II ($0.5 < SSV \leq 0.9$; moderate to severe damage). None of the buildings surveyed falls under class I ($SSV \leq 0.5$), which would be subjected to low damage. This research opens a new avenue to frame or revise proper guidelines on building constructions and design, specifically concerning landslides in the hilly terrain. It would also help the State Disaster Management Authority and Irrigation Department, Nainital, take efficient disaster risk reduction measures to reduce the landslide intensity, increase buildings' resistance, and prioritize relocation of the vulnerable households.

Keywords Balia Nala landslide · Physical vulnerability · Site-specific vulnerability · Indicator-based approach · GIS

Responsible Editor: Biswajeet Pradhan

✉ Ramesh Veerappan
rameshremote@gmail.com

Himani Tiwari
himanitiss@gmail.com

Harshita Tiwari
harshitatiwari@gmail.com

Thomas Oommen
toommen@mtu.edu

¹ Centre for Geoinformatics, Jamsetji Tata School of Disaster Studies, Tata Institute of Social Sciences (TISS), Mumbai 400088, Maharashtra, India

² Department of Hydrology, Indian Institute of Technology (IIT) Roorkee, Roorkee 247667, Uttarakhand, India

³ Geological and Mining Engineering and Sciences, Michigan Technological University, 1400 Townsend Dr, Houghton, MI 49931, USA

Introduction

Landslides covering spatial and temporal dimensions can cause excessive loss to human lives, infrastructure, and the economy (Aleotti and Chowdhury 1999; Glade and Crozier 2005; Nandi and Shakoor 2008; Del Soldato et al. 2019; Cieslik et al. 2019). These mass wasting processes are dependent on natural causes like geology (Wakatsuki et al. 2005; Zheng et al. 2021), geomorphology (Lee and Min 2001; Lan et al. 2004; Anbazhagan and Ramesh 2014), and hydrology (Sidle and Ochiai 2006), as well as triggering factors such as rainfall (Guzzetti et al. 1999; Saito et al. 2018), earthquake (Malamud et al. 2004), volcanic activity (Di Traglia et al. 2018), and anthropogenic activities (Jones et al. 2021). Vulnerability is a dynamic, inquisitive concept that describes the levels or extent of susceptibility to damage or harm, inadequacy, marginality, and frailty of social, physical, economic, environmental, and cultural systems (Adger 2006). Turner et al. (2003) described it as the probability

that the elements at risk suffer damage because of sensitivity, exposure, and lack of resilience. Thus, the highly dynamic, complex, multi-dimensional, and hazard-dependent nature of vulnerability has always made its quantification a significant challenge for the scientific communities (Fuchs et al. 2007). Still, it is an intrinsic criterion for risk estimation, assessment, and reduction. The physical vulnerability is quantified on a scale of 0 (no damage) to 1 (total damage) (Quan Luna et al. 2011; Guillard-Gonçalves et al. 2016; Papathoma-köhle et al. 2017) as it gives an idea about the degree of loss to elements at risk like buildings and roads due to hazard of some magnitude in an area. In the context of landslide hazard, the magnitude of damage to the infrastructures and buildings is a function of characteristics and location of the buildings, type of landslides and their frequency of occurrence, their intensity (quantified as landslide velocity), and magnitude (Dai et al. 2002; Thennavan et al. 2016). Different challenges exist in physical vulnerability assessment due to types of landslide movements, limited availability of the damage data, and assignment of scores as per expert's opinion to calculate the resistance of the buildings, which restricts and limits the performance of the vulnerability model (Uzielli et al. 2015; Guillard-Gonçalves et al. 2016). Despite the challenges, the quantitative vulnerability assessment approaches are gaining momentum and attention amongst the researchers. It can calculate and assess the losses and damage occurred due to the landslide hazard though with limitations (Peng et al. 2015).

The Himalayan terrain is highly prone to landslides constituting about 70% of the world's tragic and fatal landslides (Dikshit et al. 2020). Also, active geotectonics concomitant with slope failures have resulted in a massive increase in the mass wasting activities in the region (Paul and Mahajan 1999; Sah et al. 2018). The region encounters abundant rainfall during the monsoons and is one of the key triggering factors for landslide initiation (Dikshit et al. 2020). Nainital township located in the lower Himalaya of the Kumaon region of Uttarakhand has been affected by major calamitous slope failures in the past in areas like Sher-ka Danda, Kailakhan, and Balia Nala and are still prevalent in the region as studied and documented by Hukku et al. (1974), Bhandari (1987), Valdiya (1988), Sharma (2006), Pande and Pande (2008), Kotlia et al. (2009), Gupta et al. (2016), Kumar et al. (2017), Sah et al. (2018), Yhokha et al. (2018), Kuri et al. (2018), Vaid et al. (2019), Khanduri et al. (2019), and Deyet al. (2020).

Balia Nala is one of the active and significantly high landslide hazard zones of Nainital town (Kuri et al. 2018; Vaid et al. 2019). The landslides on the right side of Balia Nala were first recorded back on August 17, 1898, which was triggered after 8 days of continuous rainfall measuring 102 cm (Middlemiss 1898). In September 2014, the Rais Hotel colony located on the right side of Balia Nala was affected by a cataclysmic landslide following the intermittent rainfall. Also,

before the landslides, cracks were noticed in the buildings and the ground, indicating continuous slow movement of the slopes (Gupta et al. 2016). The fury of Balia Nala landslide due to the excessive rainfall in September 2018 was to the extent that it wiped away 3–4 houses, destroyed the roads in the nearby area, and in light of these events, 17 households were given notices to vacate and shift to a new location (Khanduri et al. 2019). Considering these devastating landslide events, the region's risk to life and infrastructure has escalated. Moreover, the haphazard constructions in the area, specifically over the landslides' crown, have further exacerbated the physical vulnerability to the landslides.

Hence, the objective of the present study is to characterize the Balia Nala landslide and assess the site-specific physical vulnerability of the buildings lying on its slope. The significant portion of this research focuses on quantifying the site-specific physical vulnerability of 63 households in the Balia Nala area. This quantification would help the concerned authorities (like State Disaster Management Authority, Uttarakhand and Irrigation Department, Nainital) to undertake Disaster Risk Reduction (DRR) activities focused on reducing the intensity of landslide by implementing sustainable measures in the study area. Also, undertake efficient remedial measures for the highly vulnerable households and prioritize their relocation. The study provides a path to revise/frame the guidelines on building constructions and design specifically concerning landslides in the study area. The study also highlights the need to constantly monitor the growing illegal construction to reduce disaster risk and promote sustainable development. The Geographic Information System (GIS) is used to map and calculate the areal extent of the Balia Nala landslide. The site-specific physical vulnerability of the buildings was estimated using an indicator-based approach adopted by Singh et al. (2019a, b).

Previous studies

Papathoma-köhle et al. (2017) reviewed and discussed three varied approaches, viz., damage or vulnerability matrix, vulnerability curves, and an indicator-based approach for assessing the physical vulnerability of buildings specifically for debris flows. The damage or vulnerability matrix approach was first proposed by Leone et al. (1995) and resulted in the vulnerability value from 0 to 1 using damage states based on the process intensity. A new methodology for damage probability matrix by Erenner and Düzgün (2011) also incorporated remote sensing and GIS for vulnerability assessment. Damage matrices on the basis of past events (Bründl et al. 2009) were also proposed. Jakob et al. (2012) developed a damage probability matrix by calculating the intensity index of the landslide and correlated it with the damage of the buildings using the HAZUS software. A matrix for Reinforced

Concrete (RC) and non-Reinforced Concrete (non-RC) buildings based on impact pressure was proposed by Kang and Kim (2016). To study the effects of diverse variables on the bearing capacity of footings on soil slopes, Satvati et al. (2020) used a laboratory approach using three-dimensional geosynthetics called expandable braided sleeve and geogrid. Damage/vulnerability matrices clarify the relationship between the process and the consequence; hence is easily understandable by the common people. However, its subjective nature of assessment poses one of the significant limitations (Papathoma-köhle et al. 2017).

The vulnerability curve is a quantitative method to assess physical vulnerability and is mainly focused on quantifying damage loss of buildings into a monetary value. Fuchs et al. (2007) were the first to underscore the importance of this method and derived the vulnerability curves using the intensity of debris flow landslide and damage ratio of the buildings in the Alps, Austria. Vulnerability curves were also integrated into landslide vulnerability studies by Mavrouli et al. (2014) and Uzielli et al. (2015) for prestressed-concrete buildings. Finally, Chen et al. (2020) proposed a methodology to assess the physical vulnerability of the masonry buildings exposed to the effects of slow-moving landslides by using this method.

An indicator-based approach for assessing physical vulnerability has recently gained importance. Its process includes selecting the physical vulnerability indicators, identifying the variables, assigning weights followed by the final assessment. Papathoma-Köhle et al. (2007) were the first to attempt this approach to assess physical vulnerability for the hilly region hazards by assigning weights to the indicators based on expert's judgement. Li et al. (2010) used an indicator-based approach with susceptibility of elements at risk and landslide intensity as inputs for assessing the physical vulnerability of the infrastructure. Kappes et al. (2012) further improved this method without considering the landslide's intensity. Physical vulnerability and the probable losses of the buildings affected by the shallow landslides were assessed by Silva and Pereira (2014) at a municipality (regional level) using this approach by combining the 'resistance' and 'intensity of process' parameters. Du (2012) and Du et al. (2016) also used an indicator-based approach to assess the vulnerability of buildings due to landslides. Following the methodology of Du (2012), vulnerability assessment was conducted by Guo et al. (2020) using the same approach. Thennavan et al. (2016) carried out a vulnerability assessment of buildings in the high hazard landslide-prone area in the Nilgiris district using thematic layers of indicators related to buildings and calculated the vulnerability scores using empirical formulas scripting in a GIS environment. Ettinger et al. (2016) also used an indicator-based approach and further analysed the relationship between the vulnerability indicators and damage data using logistic regression. A study by Singh et al. (2017) reviewed several studies on qualitative

and quantitative vulnerability approaches. It proposed a new methodology that considered structural details and typology of the buildings as indicators to assess the physical vulnerability. A study by Singh et al. (2018) adopted a modified semi-quantitative approach in which landslide intensity was quantified using velocity, volume, and building's resistance of around 71 buildings in the Joshimath block of Uttarakhand, India. Physical vulnerability assessment of the buildings exposed to the rockfall hazard was conducted by Singh et al. (2019a, b) using empirical formula applied in Li et al. (2010). An indicator-based approach using 15 different indicators was used to assess the vulnerability to buildings at a site-specific scale in the ward of Chamoli district, India (Singh et al. 2019a, b). Bera et al. (2020) adopted indicator-based approach and used the Fuzzy-AHP approach to calculate the resistance scores of the buildings by considering the geomorphological conditions and applied it to 332 buildings in the high and active landslide hazard zone in the Kalimpong area.

The present study incorporates the methodology adopted by Singh et al. (2019a, b) for assessing the site-specific vulnerability of the buildings located in Balia Nala, Nainital, Uttarakhand. The indicator-based approach is preferred in this study over the damage/vulnerability matrix methodology due to its highly subjective nature of assessments. Moreover, one of the major limitations of vulnerability curves is that it is not applicable for the regions with different building types, and for obtaining a result, there is a need for a greater number of affected buildings (Papathoma-Köhle et al. 2017). Not many damaged/affected buildings were there in our study area due to the landslide. Hence, indicator-based approach was finalized, and the methodology adopted by Singh et al. (2019a, b) has been applied due to the similarity in the study area and landslide type (debris flow).

Study area

Nainital town, a famous hill station, is one of the flag bearers of the tourism industry of Uttarakhand. Ayarpatta, Sher-ka-Danda, Naina Peak, and Deopatha are the prominent hills surrounding the Naini Lake (Khanduri et al. 2019). About half of the township area is covered with debris accumulated due to the frequent mass wasting activities in the region (Valdiya 1988). The study area, Balia Nala, is located at 29°22'26.13"N latitude and 79°27'55.53"E longitude at an elevation of 1872 m in the Hari Nagar ward of Nainital town with the ward's population of 2825 (Census of India, 2011) (Fig. 1). Mass wasting activities are common and frequent along both sides of the Nala, which flows in the S-E direction and is a natural outlet of Nainital Lake (Kuri et al. 2018). The continuous and rampant toe erosion of the Balia Nala landslide and burgeoning haphazard construction activities have added to the causes of slope instability in the

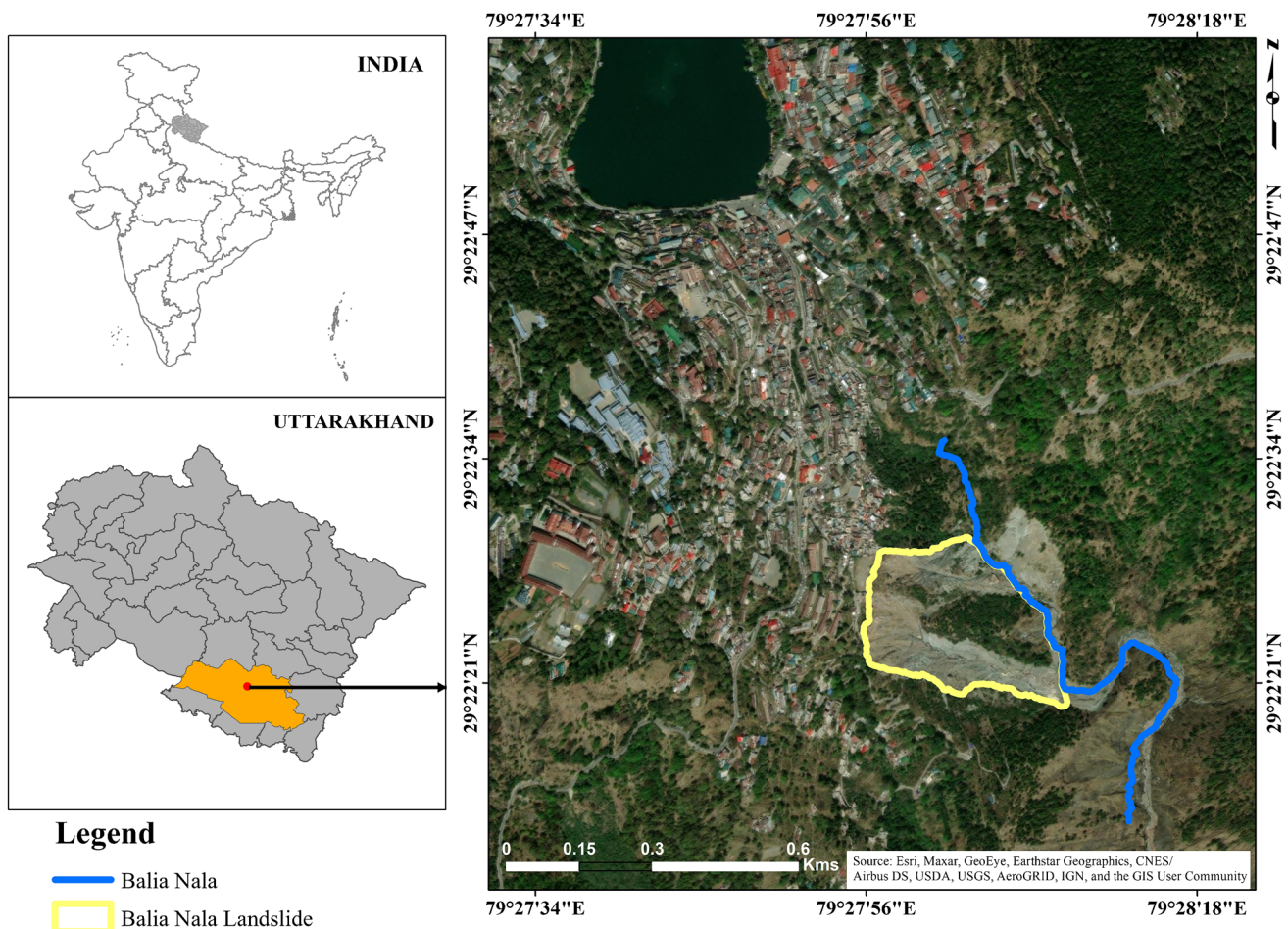


Fig. 1 Study area—Balía Nala, Nainital, India, area with the landslide demarcated (source: Google Earth satellite imagery)

area (Khanduri et al. 2019; Gupta et al. 2016; Rautela et al. 2014). Field photographs of the exposed and affected buildings to the Balía Nala landslide are shown in Fig. 2.

The township experiences salubrious summers and extremely cold winters. The temperature during the summers varies in the range of 10 to 28 °C and can even touch below 0 °C. In the monsoons (June to September), the area experiences moderate to heavy rainfall, which is one of the most important triggering factors for landslide reactivation in the area. As per the Irrigation Department of Nainital, the year 2010 recorded the highest average monsoon rainfall of about 1027 mm between the years 2005–2019. An increase in landslide activities was witnessed in the region following this heavy rainfall.

Geological setting

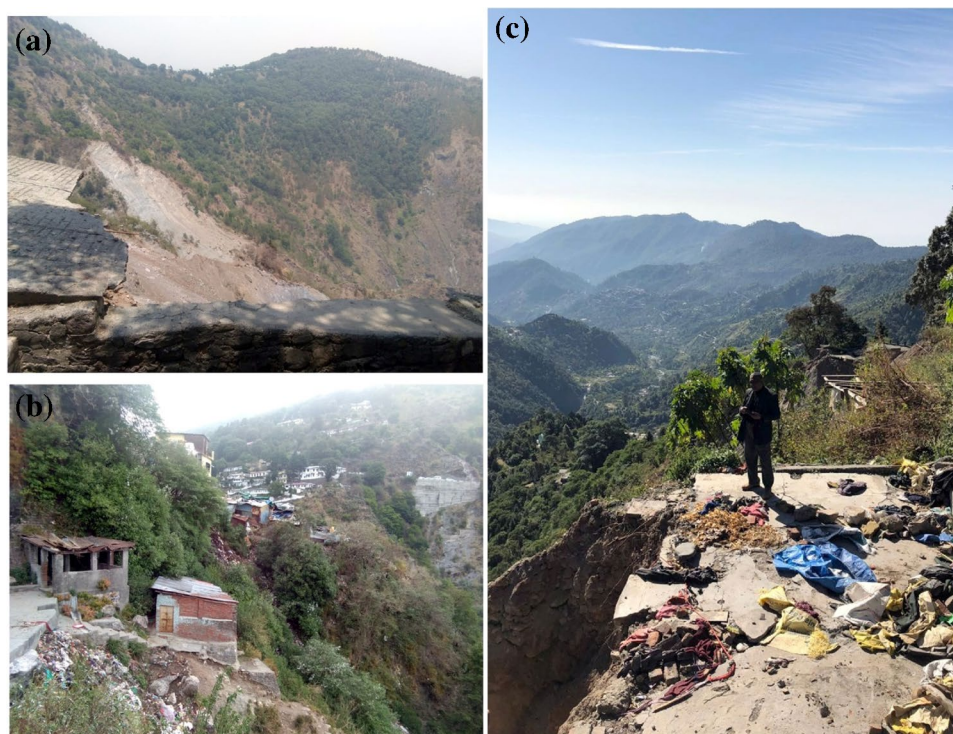
Nainital town majorly constitutes rocks like slate, shale, and limestone, which belong to the various formations viz. Krol, Blaini, and Tal of the Lesser Himalaya. The Krol group of rocks dominate in the Nainital township and mainly constitute grey and blue dolomitic limestone, argillaceous

limestone, calcareous slate, siltstone, greywacke etc. The eastern and north-eastern parts of the Nainital Lake comprises mainly of the Blaini formation in which conglomerates associated with dolomite limestone, quartzitic, and purple slate dominate. In contrast, the Tal formation is majorly found near the south-western side of the lake and represented by fine-grained sandstone and siltstone, pyritic shale, and slate (Gupta et al. 2016). The area witnesses many faults, thrusts, and folds which transect the region of which the Nainital Lake fault trending in the NW–SE direction cuts the Main Boundary Thrust (MBT) and extends to the Balía Nala and is responsible for the weak geological setup (Valdiya 1988). It has resulted in weathering, further increasing the fragility of the dominantly found rocks in the area like slate, shale, and limestone leading to landslides.

Methodology and data collection

Quantitative vulnerability assessment for the hazards is recommended and preferred over qualitative assessments. It can evaluate or measure the losses, eliminating the

Fig. 2 Field photographs show Balia Nala landslide and its impact: **a** view of landslide, **b** and **c** exposed and affected households



communication gap between technical or political groups for better decision-making (Uzielli et al. 2008). The methodology developed by Singh et al. (2019a, b) is applied additionally with the aid of GIS to a different site, i.e. Balia Nala, a debris flow type landslide located in the foothills of the Kumaon outer Himalaya. The following steps have been followed to quantitatively assess the physical vulnerability of the buildings in the close periphery around the crown of the Balia Nala landslide (Fig. 3).

Spatial mapping of households and selection of building vulnerability indicators

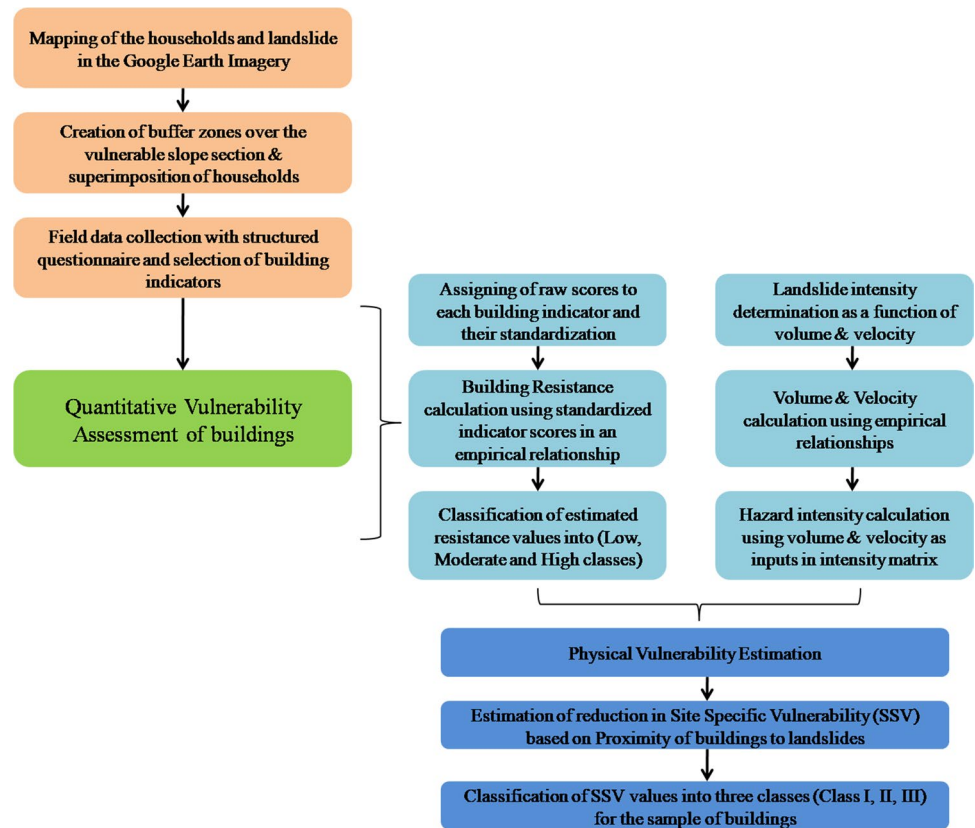
A thorough field survey was carried out with the concerned authorities of the Irrigation Department, Nainital. The details of the hazard occurrences were gathered from literature surveys, newspaper articles, and most importantly, after the interaction with the local communities. Google Earth imageries of the years 2010, 2015, and 2019 were digitized to understand the areal extent and geometry of the Balia Nala landslide. Also, around 595 households visible in the Google Earth imagery of the year 2019 were mapped, which was followed by the creation of two buffer zones of 0–200 m and 200–400 m over the vulnerable slope section of the landslide and the digitized households were superimposed over the buffer zone. A total of 63 samples of households were randomly selected within these two buffer zones, and this pre-field map was taken as the footprint map for field data collection. Further, the

building vulnerability indicators such as roof design and material, foundation material, type of construction (fully/partially engineered, non-engineered, and marginally engineered), and the height of the building, on which the resistance of a building depends, were taken into consideration. For the present study, most of the indicators are selected from the study by Singh et al. (2019a, b) due to the similarity of the terrain conditions of our study region in combination with the Indian Standard codes, viz., Indian Standard Code 14,804 on ‘Siting, Design and Selection of Materials for Residential Buildings in Hilly Areas’; National Building Code of India, 2005 (Group 1, ANNEX G, Clause 12.24) and National Building Code of India, 2016 (Group 1, ANNEX F, Clause 17) on ‘Special Requirements for development Planning in hilly areas’, literature surveys and based on the availability of data. Thus, 15 building indicators were selected, and a structured questionnaire was prepared based on those indicators as clearly tabulated in Table 1. The ground truth information was then collected with the help of the questionnaire by interviewing the inhabitants of the 63 selected sample households and the information gathered was compiled together to assess the vulnerability of the buildings.

Physical vulnerability assessment of the buildings

Physical vulnerability is considered in this study as a function of landslide intensity and building resistance. After the indicators were selected, raw scores were assigned

Fig. 3 Methodology flowchart



based on interviews with locals, Indian Codal guidelines for hilly terrain (IS 14458 (Part 2) 1997; BIS 2016; IS 14804 2000), and a thorough literature review (Papathoma-Köhle et al. 2007; Singh et al. 2019a, b; Joshi et al. 2019). The raw score of 1 represents the ‘most vulnerable’ category, and the increasing raw scores signify the decrease in building vulnerability. These raw scores were further standardized in the range 0 to 1 by applying the formula proposed by Voogd (1983) as shown in Eq. (1).

$$\text{Standardized Score} = \frac{\text{Raw Score}}{\text{Maximum Raw Score}} \quad (1)$$

These standardized resistance scores of the 15 indicators were used as inputs in the resistance formula (Eq. 2) applied by Li et al. (2010) for calculating the resistance of the buildings, which plays a crucial role in vulnerability assessment and can be defined as the capacity of the structure to withstand the hazard of a given intensity. Further, the estimated resistance values were classified into three categories for a landslide-prone region in hilly terrains with its sliding material as debris by Singh et al. (2019a, b) and is presented in Table 2.

$$R = \left(\prod_{i=1}^{n_s} \xi_i \right)^{\frac{1}{n_s}} \quad (2)$$

where R indicates the resistance capability of the building, ξ_i is the i th standardized resistance score of the building for a specific indicator, and n_s indicates the total number of selected indicators.

Another important factor considered for assessing the vulnerability and the magnitude of loss is the landslide’s intensity, which depends on the landslide’s moving mechanism and its type (Solari et al. 2020). Hungr (1997) defined it as the landslide’s level of destructiveness, which can be measured using a variety of parameters such as velocity, volume, deposition height, debris depth, deformation, pressure, momentum, kinetic energy (per unit area), mass thickness, run-out distance, peak discharge, and the area affected by the landslides (Ojeda-Moncayo et al. 2004; Singh et al. 2018). In the present study, two parameters, viz., the volume of the landslide (V) and its velocity (U) used by Cardinali et al. (2002), are considered for quantifying the landslide intensity (I_s) as shown in Eq. 3.

$$I_s = f(U, V) \quad (3)$$

Volume is an essential geometrical parameter that controls the run-out distance, the affected area, and the potential damages incurred on elements at risk (Jaboyedoff et al. 2020). It can be estimated using the average depth of landslide and surface area, but empirical formulae defining the relationship between landslide volume and area are generally

Table 1 Questionnaire for physical vulnerability assessment (source: Papatoma-Köhle et al. 2007; IS 14458 (Part 2) 1997; BIS 2016; IS 14804 2000; Singh et al. 2019a, b; Joshi et al. 2019)

Building location (coordinates) building ID		
S. no	Indicators	
1	Year of construction	
2	No. of floors	
3	Roof material and design	Flat roof in local material/unreinforced concrete Pitched roof in slate/local material Pitched/gabled roof in tin/GCI sheets Flat roof in RC
4	Structural typology (material)	Stone masonry Unreinforced brick masonry Reinforced concrete Other material (tin, wood)
5	Surrounding wall of the building	No wall Low/medium wall Strong high wall
6	Horizontal configuration	Regular/irregular
7	Distance between windows and doors from each other greater than or equal to 1 m	Yes No
8	Distance between two houses from each other equal to or greater than 1 m	Yes No
9	Presence of windows and openings in the building facing the steep slope	Yes No
10	Surrounding ambience	Built-up Built-up with forest
11	State of maintenance	(a) Cracks in the structure (reason) (b) Ground settlement (c) Water seepage in building (yes/no)
12	Type of construction	Non-engineered Marginally engineered Engineered
13	Retrofitted building	Yes No
14	Presence of warning signs of landslides	Yes No
15	Position of building from the slope	

Table 2 Resistance classes (source: Singh et al. 2019a, b)

S. no	Class	Resistance range
1	Low	$R \leq 0.5$
2	Moderate	$0.5 < R \leq 0.9$
3	High	$0.9 < R \leq 1$

adopted (Guzzetti et al. 2009). Thus, the area of landslide using Google Earth imagery shown in Fig. 1 was calculated in ArcMap software, and the volume was evaluated using the empirical formula proposed by Guzzetti et al. (2009) for debris flow as shown in Eq. 4.

$$V = 0.074 * A_L^{1.450} \tag{4}$$

Velocity is another crucial parameter that governs the flow momentum and the kinetic energy based on which the intensity of landslide can be determined. The methods developed for determining the velocity range from statistical-empirical relationships to three-dimensional run-out models like RAMMS, DAN3D, MassMov2D, and NGI (Mcdougall 2014). In the study, the already established empirical relationship by Rickenmann (1999) as shown in Eq. 5 has been used to calculate the debris flow velocity as our study also focuses on debris flow landslides.

Once the volume and velocity are evaluated, the intensity is estimated using the intensity matrix proposed by Singh et al. (2018).

$$U = 2.1Q_p^{0.33}S^{0.33} \tag{5}$$

where ‘ U ’ is the landslide velocity, ‘ S ’ represents the local slope, and ‘ Q_p ’ represents the peak discharge of boulder material and is given by $Q_p = 0.1V^{0.83}$ where V represents the volume.

Once the building resistance and the landslide intensity are quantified and calculated, the formula proposed by Li et al. (2010) as shown in Eq. 6 is further used for the calculation of the physical vulnerability (PV) of the sample buildings.

$$PV = f(I_s, R) = \begin{cases} 2 \frac{I_s^2}{R^2} & \frac{I_s}{R} \leq 0.5 \\ 1 - \frac{2(R-I_s)^2}{R^2} & 0.5 < \frac{I_s}{R} \leq 1.0 \\ 1.0 & \frac{I_s}{R} > 1 \end{cases} \quad (6)$$

The proximity of these households to the landslide is then taken into consideration by using the 20-m contour interval derived using ALOS PALSAR digital elevation model (DEM) and the percentage decrease in the physical vulnerability of the respective households due to proximity from the crown of the Balia Nala landslide (Table 3), by using the empirical relationship proposed by Singh et al. (2019a, b) as shown in Eq. (7).

$$SSV = PV - A \quad (7)$$

Table 3 Percentage reduction in physical vulnerability of buildings due to proximity from Balia Nala landslide (source: Singh et al. 2019a, b)

Distance from Balia Nala landslide (in m)	Percentage reduction in physical vulnerability
0–20 m	0
21–40 m	5
41–60 m	10
61–80 m	15
81–100 m	20
101–120 m	25
121–140 m	30
141–160 m	35
161–180 m	40
181–200 m	45

Table 4 Site-specific vulnerability classes (source: Singh et al. 2019a, b)

Class	Range of SSV	Probable damage
I	≤ 0.5	Low: In this case, there will be very less chance of damage and if it occurs, it would require normal repairing and low cost
II	$0.5 < SSV \leq 0.9$	Moderate to severe: In this, immediate evacuation would be required since the functionality of the building would be compromised. The costs involved in retrofitting would be high
III	$0.9 < SSV \leq 1$	Very severe to complete: The buildings cannot be retrofitted or fixed, hence would require the clearing of site

where ‘ SSV ’ represents the site-specific vulnerability, ‘ PV ’ represents the physical vulnerability, and ‘ A ’ represents the percentage reduction in physical vulnerability with distance. The obtained site-specific physical vulnerability was further classified into three classes (class I, class II, and class III) as per the classification proposed by Singh et al. (2019a, b) and is shown in Table 4.

Results

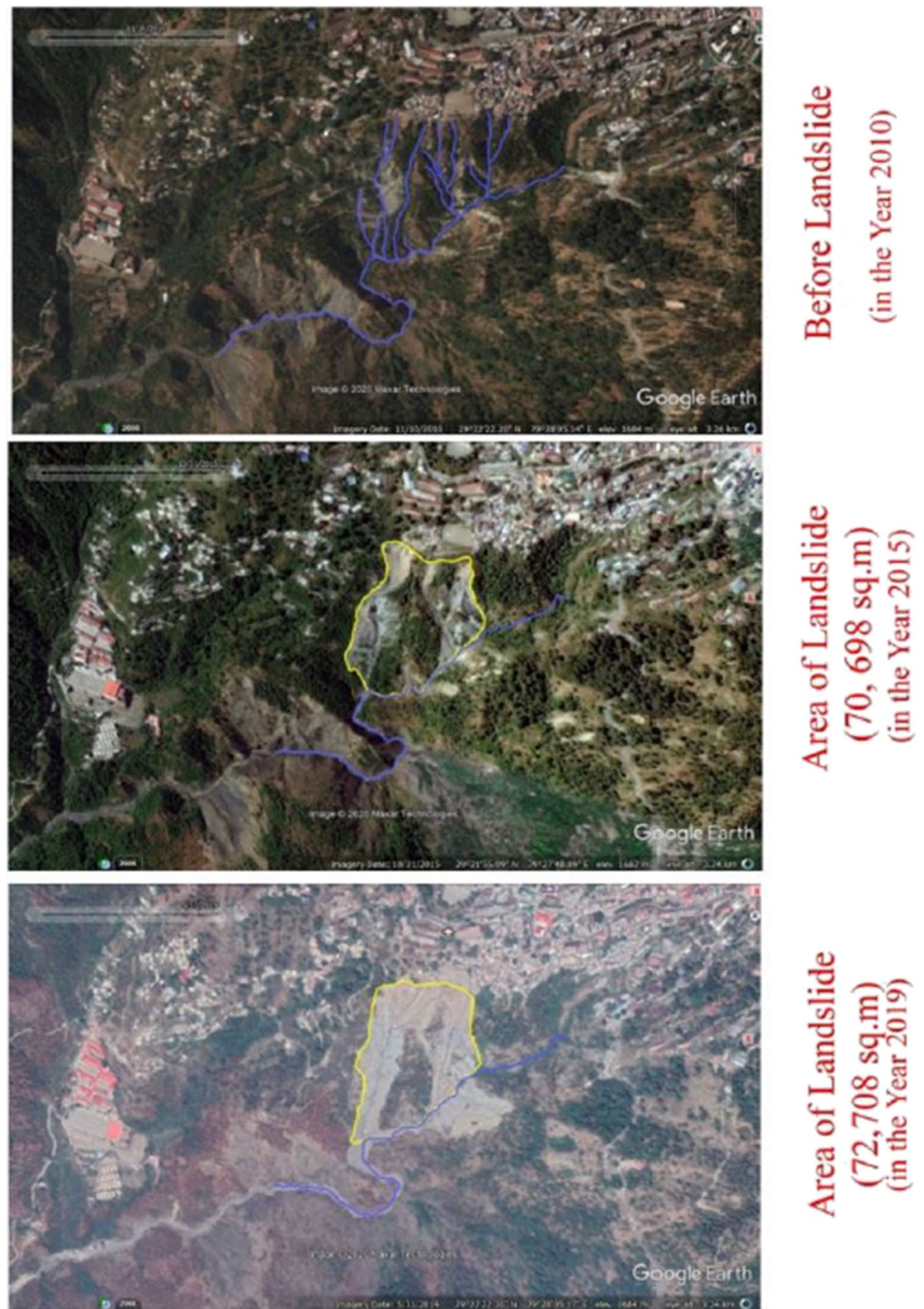
Characteristics of Balia Nala landslide

Balia Nala landslide is a debris flow type landslide with two seepages present on the face of the slide. It is retrogressive and widening in nature with its progression towards the northern direction and has a maximum length of about 447 m and a maximum width of 282 m. The slide’s crown and toe are located at an elevation of $EL \pm 1820$ m and $EL \pm 1560$ m respectively and face towards the north-eastern direction with a minimum slope of 3° , a maximum slope of 68° , and an average slope of 32° . The landslide has been prominent in the region since the twentieth century but has shown major reactivation activity after 2010 (Gupta et al. 2016). Mapping of the landslide region using the Google Earth images of the years 2010, 2015, and 2019 showed an increase of landslide area from 70,698 to 72,708 m^2 (a rise of 2010 m^2) within 5 years (2015 to 2019) (Fig. 4). Thus, triggering factors like rainfall, Balia Nala fault, which passes through the toe of the slide, proximity to drainages, presence of seepages, higher natural slope conditions, haphazard and unplanned construction in the landslide area have resulted in the increasing instability of the Balia Nala slope.

Estimation of resistance of each building

Resistance plays a vital role in vulnerability assessment and is the capacity of the structure to withstand the hazard of a given intensity. Based on the extensive field survey of the 63 buildings with the help of the structured questionnaire, it was found that the majority of the surveyed buildings in the region were constructed between the years (R1) 1901–2000 and are low rise buildings with two floors (R2) and have

Fig. 4 Progression and areal extent of Balia Nala landslide from 2010 to 2019



pitched roofs in the tin (R3) with no surrounding wall (R5). The recent constructions are made up of reinforced concrete (40%), whereas the older constructions are made up of stone masonry and unreinforced brick masonry (R4), which contribute to around 54%. The distance between 2 buildings (R7) and the distance between windows and doors (R6) is less than 1 m in 84% and 59% of the surveyed buildings, which indicates the haphazard construction in the study area. Openings on the side facing the slope (R8) could be found in 57% of the buildings and 92% having no forest or trees cover

(R9) in its vicinity, which infers burgeoning urbanization in the region. In 18% of the cases, cracks were noticed in the old buildings and the ground settlement (R10), and only 35% of the surveyed buildings were retrofitted timely (R12); 73% of buildings showed no warnings of landslides (R13). Regular horizontal configuration (R14) contributes to the lesser vulnerability of the buildings; from the survey, 75% of the buildings showed this type of configuration. Of the surveyed households, 54% were engineered and belonged to the category of either newly constructed buildings or the

buildings constructed during the British Raj (R11). Also, a maximum percentage of buildings were found at a distance of 51–100 m from the landslide slope (R15). The percentage of surveyed households of vulnerability indicators is given in Table 5. The raw scores assigned to the different physical indicators and their respective standardized resistance scores calculated using Eq. 1 is shown in Table 6. Likewise, Table 7 represents the values of resistance factors and the overall resistance (R) of the surveyed buildings calculated using Eq. 2. The following result concluded from the above calculations that out of the 63 buildings, about 89% of them belonged to the category of ‘moderate resistance class’; 11% fell under the category of ‘low resistance’; and none of the surveyed buildings fell in the ‘high resistance’ category. The buildings falling under the various resistance classes are shown in Fig. 5.

Estimation of the intensity of landslide

Landslide intensity is the other important parameter taken into consideration for vulnerability quantification which is further taken as a function of landslide’s volume and velocity. The estimated area of the Google Earth imagery dated 31/05/2019 is calculated to be 72,708 m² with the aid of GIS; this value is further used in Eq. 4 for volume estimation of the Balia Nala landslide, which is obtained as 828,945 m³ and comes under the ‘high’ category (Sarkar et al. 2015). The velocities at the minimum, maximum, and average slopes were computed using Eq. 5 after classifying the slope of the landslide using ALOS PALSAR DEM (12.5 m) and are shown in Fig. 6. The values of landslide velocity estimated for minimum (3°), maximum (68°), and average (32°) slopes are 15.5 m/s, 43.4 m/s, and 33.8 m/s, respectively. Hence, the velocity of landslide lies in the range of 15.5 to 43.4 m/s, which belongs to the ‘extremely rapid’ category as proposed by Cruden and Varnes (1996). Landslide intensity is further categorized as ‘very high’ on a scale of 0 to 1; its value is 1 by using the landslide intensity matrix proposed by Sarkar et al. (2015).

Physical vulnerability of individual building and its quantification at site-specific scale

Physical vulnerability is calculated by putting together the values of resistance of individual buildings and landslide intensity value of 1 in Eq. 6, which results in a uniform physical vulnerability of value ‘1’ for all the surveyed buildings despite varying resistances of the buildings as the estimated landslide intensity is very high. To have a better understanding of the vulnerability quantification, the site-specific vulnerability of the individual buildings is calculated using Eq. 7, and the results are tabulated in Table 8 with a categorization of the buildings into three classes; class I, class

II, and class III as proposed by Singh et al. (2019a, b). The following observations were made; out of the 63 surveyed buildings, 44% of them fall under class III ($0.9 < SSV \leq 1$; very severe to complete), which infers that in the case of any severe future landslide, the buildings would get damaged with no scope of retrofitting. About 56% of them fall under class II ($0.5 < SSV \leq 0.9$; moderate to severe), which signifies that the functionality of the buildings would be compromised and hence very high costs would be required for retrofitting when struck by a severe landslide, whereas none of the buildings surveyed falls under class I ($SSV \leq 0.5$), which in the future would be subjected to low damage (Fig. 7). It shows that the buildings are highly vulnerable based on the proximity to the Balia Nala landslide. Few field photographs of the surveyed households are shown in Fig. 8.

Discussion

This study aims to assess the physical vulnerability of the 63 sample households using an indicator-based approach and GIS aid. The evaluation of physical vulnerability is an outcome of the complete process like selecting 15 building indicators, field survey, calculation and standardization of raw scores, calculation of resistance and intensity of the households. The final resistance calculated as a function of standardized resistance score shows that the majority of the buildings (89%) provide ‘moderate resistance’ ($0.5 < R \leq 0.9$) and 11% are ‘low resistant’ ($R \leq 0.5$). The least resistance evaluated was 0.44 (building ID H12) and the highest was 0.88 (building ID H57). As per the field observation of the study area, the majority of the households are illegally built, and they belong to people with a poor socio-economic background. Most of the households constructed in the encroached area were made of wood, tin, and bricks and were non-engineered. Owing to this fact, after considering all the vulnerability indicators, none of the households provides high resistance capability ($0.9 < R \leq 1$) and falls in the ‘moderate’ or ‘low’ resistance classes.

The other most crucial parameter is the calculation of landslide intensity, which is calculated as a function of velocity and volume in this study. The velocity of landslide obtained ranges between 15.5 and 33.8 m/s (falls under ‘extremely rapid’ category), and the volume amounts to 8,28,945 m³ (falls under ‘high’ category). Using a landslide intensity matrix, the landslide intensity obtained is ‘1’ and falls under the ‘very high’ category. Damaged roads, demolished and abandoned houses, and continuous subsiding of grounds in the study area are all indicators of this result. It is a very alarming issue and urgently requires the implementation of suitable and sustainable remedial measures in this hill slope. The resistance and landslide intensity obtained are further used to evaluate physical vulnerability. This study got a constant physical vulnerability value

Table 5 Percentage of surveyed households of vulnerability indicators

Indicators	Category notation	Categories	Percentage of households
Year of construction (R1)	R1a	Before 1900	5%
	R1b	1901–1950	27%
	R1c	1951–2000	40%
	R1d	2001–2019	28%
No. of floors (R2)	R2a	Single storey	30%
	R2b	Low rise (2 floors)	37%
	R2c	Medium (3, 4 floors)	30%
	R2d	High rise (5,6 and more)	3%
Roof material and design (R3)	R3a	Flat roof in local material/unreinforced concrete	22%
	R3b	Pitched roof in slate/local material	3%
	R3c	Pitched/gabled roof in tin/GCI sheets	56%
	R3d	Flat roof in RC	19%
Structural typology (R4)	R4a	Stone masonry	33%
	R4b	Unreinforced brick masonry	21%
	R4c	Reinforced concrete	40%
	R4d	Other material (tin, wood etc.)	6%
Surrounding wall (R5)	R5a	No wall	73%
	R5b	Low/medium wall	16%
	R5c	Strong high wall	11%
Distance between windows and doors equal to or greater than 1 m (R6)	R6a	Yes	59%
	R6b	No	41%
Distance between two houses from each other greater than or equal to 1 m (R7)	R7a	Yes	16%
	R7b	No	84%
Presence of windows and openings in the building facing the slope (R8)	R8a	Yes	57%
	R8b	No	43%
Surrounding ambience (R9)	R9a	Only built-up	92%
	R9b	Built up with forest and trees	8%
State of maintenance (R10)	R10a	Excellent	1%
	R10b	Good	59%
	R10c	Medium	22%
	R10d	Poor	18%
Type of construction (R11)	R11a	Engineered	54%
	R11b	Marginally engineered	11%
	R11c	Non-engineered	35%
Retrofitted building (R12)	R12a	Yes	35%
	R12b	No	65%
Presence of warning signs of landslide (R13)	R13a	Yes	27%
	R13b	No	73%
Horizontal configuration (R14)	R14a	Regular	75%
	R14b	Irregular	25%
Position of building from the slope (R15)	R15a	0–50 m	14%
	R15b	51–100 m	28%
	R15c	101–150 m	6%
	R15d	151–200 m	13%
	R15e	201–250 m	8%
	R15f	251–300 m	1%
	R15g	301–350 m	11%
	R15h	351–400 m	19%

Table 6 Raw scores and resistance factor

Indicators	Category notation	Categories	Raw score	Resistance factor
Year of construction (R1)	R1a	Before 1900	1	0.25
	R1b	1901–1950	2	0.5
	R1c	1951–2000	3	0.75
	R1d	2001–2019	4	1
No. of floors (R2)	R2a	Single storey	4	1
	R2b	Low rise (2 floors)	3	0.75
	R2c	Medium (3, 4 floors)	2	0.5
	R2d	High rise (5,6 and more)	1	0.25
Roof material and design (R3)	R3a	Flat roof in local material/unreinforced concrete	1	0.33
	R3b	Pitched roof in slate/local material	1	0.33
	R3C	Pitched/gabled roof in tin/GCI sheets	2	0.67
	R3d	Flat roof in RC	3	1
Structural typology (R4)	R4a	Stone masonry	1	0.33
	R4b	Unreinforced brick masonry	2	0.67
	R4c	Reinforced concrete	3	1
	R4d	Other material (tin, wood etc.)	1	0.33
Surrounding wall (R5)	R5a	No wall	1	0.33
	R5b	Low/medium wall	2	0.67
	R5c	Strong high wall	3	1
Distance between windows and doors equal to or greater than 1 m (R6)	R6a	Yes	2	1
	R6b	No	1	0.5
Distance between two houses from each other greater than or equal to 1 m (R7)	R7a	Yes	2	1
	R7b	No	1	0.5
Presence of windows and openings in the building facing the slope (R8)	R8a	Yes	2	1
	R8b	No	1	0.5
Surrounding ambience (R9)	R9a	Only built-up	1	0.5
	R9b	Built up with forest and trees	2	1
State of maintenance (R10)	R10a	Excellent	4	1
	R10b	Good	3	0.75
	R10c	Medium	2	0.5
	R10d	Poor	1	0.25
Type of construction (R11)	R11a	Engineered	3	1
	R11b	Marginally engineered	2	0.67
	R11c	Non-engineered	1	0.33
Retrofitted building (R12)	R12a	Yes	2	1
	R12b	No	1	0.5
Presence of warning signs of landslide (R13)	R13a	Yes	2	1
	R13b	No	1	0.5
Horizontal configuration (R14)	R14a	Regular	2	1
	R14b	Irregular	1	0.5
Position of building from the slope (R15)	R15a	0–50 m	1	0.125
	R15b	51–100 m	2	0.25
	R15c	101–150 m	3	0.375
	R15d	151–200 m	4	0.5
	R15e	201–250 m	5	0.625
	R15f	251–300 m	6	0.75
	R15g	301–350 m	7	0.875
	R15h	351–400 m	8	1

'1' represents the most vulnerable

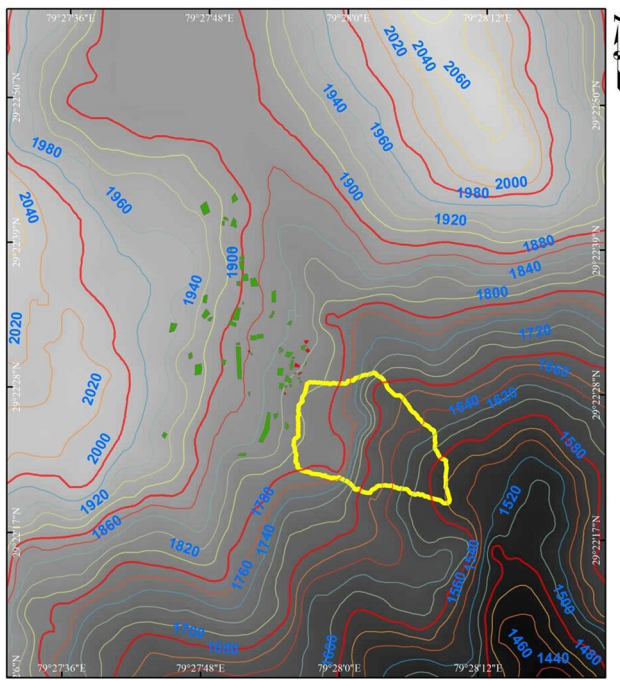
Table 7 Resistance (*R*) of each building in the study area

Building ID	R1	R2	R3	R4	R5	R6	R7	R8	R9	R10	R11	R12	R13	R14	R15	<i>R</i>
H1	0.75	1	0.67	0.67	0.33	1	0.5	0.5	0.5	0.5	0.67	0.5	1	1	0.125	0.58
H2	0.75	1	0.33	0.33	0.33	0.5	0.5	0.5	0.5	0.5	0.33	0.5	1	1	0.125	0.48
H3	0.75	0.5	0.67	0.67	0.33	0.5	0.5	0.5	0.5	0.5	0.67	0.5	1	0.5	0.125	0.51
H4	0.75	0.5	0.67	1	1	1	0.5	0.5	0.5	0.75	1	0.5	1	1	0.125	0.65
H5	1	1	0.67	1	0.33	1	0.5	1	0.5	0.75	0.33	0.5	1	1	0.125	0.62
H6	0.5	0.5	0.67	0.33	0.33	1	0.5	1	0.5	0.75	0.67	0.5	0.5	1	0.125	0.55
H7	0.75	0.5	1	1	0.33	0.5	0.5	0.5	0.5	0.75	0.67	0.5	1	1	0.25	0.6
H8	0.75	1	0.33	0.33	0.33	1	0.5	1	0.5	0.5	0.33	0.5	0.5	0.5	0.25	0.5
H9	0.75	0.75	0.67	0.33	0.67	0.5	0.5	1	0.5	0.75	0.33	0.5	0.5	1	0.125	0.53
H10	1	0.5	0.33	0.67	0.33	0.5	0.5	0.5	0.5	0.25	0.33	0.5	1	0.5	0.25	0.47
H11	1	0.25	0.67	1	0.33	1	0.5	0.5	0.5	0.75	0.33	0.5	0.5	1	0.25	0.54
H12	0.75	0.5	0.33	0.33	0.33	0.5	0.5	1	0.5	0.25	0.33	0.5	0.5	0.5	0.25	0.44
H13	0.75	0.75	0.67	0.67	0.33	0.5	0.5	1	0.5	0.75	0.33	0.5	0.5	0.5	0.25	0.53
H14	1	1	0.67	0.33	0.33	1	0.5	1	0.5	0.5	0.33	0.5	1	0.5	0.25	0.56
H15	0.75	1	0.67	0.33	0.33	1	0.5	1	0.5	0.5	0.33	0.5	0.5	0.5	0.375	0.54
H16	1	0.75	1	1	0.33	1	0.5	1	0.5	0.75	1	0.5	0.5	1	0.25	0.68
H17	1	0.75	1	1	0.33	0.5	0.5	1	0.5	0.75	1	0.5	0.5	1	0.25	0.65
H18	0.75	0.5	0.67	0.67	0.33	0.5	0.5	0.5	0.5	0.75	0.33	0.5	0.5	0.5	0.25	0.5
H19	0.5	0.5	0.67	0.33	0.33	1	0.5	0.5	0.5	1	0.67	1	0.5	0.5	0.25	0.54
H20	0.75	0.5	0.67	0.67	0.33	0.5	0.5	0.5	0.5	0.75	1	1	0.5	1	0.25	0.59
H21	0.75	1	1	1	0.33	1	0.5	0.5	0.5	0.75	0.33	0.5	0.5	1	0.25	0.6
H22	0.75	0.75	0.33	0.67	0.67	0.5	0.5	0.5	0.5	0.5	0.33	0.5	1	1	0.125	0.52
H23	1	0.75	0.33	1	0.33	0.5	0.5	1	0.5	0.75	0.33	0.5	1	1	0.125	0.56
H24	1	0.75	0.33	0.67	0.33	0.5	0.5	0.5	0.5	0.25	0.33	0.5	1	1	0.125	0.48
H25	0.75	0.75	1	1	0.33	1	0.5	0.5	0.5	0.75	0.33	0.5	1	0.5	0.25	0.59
H26	0.25	1	0.67	0.33	0.33	1	1	0.5	0.5	0.5	1	0.5	1	1	0.25	0.58
H27	0.25	1	0.67	0.33	0.33	1	1	1	0.5	0.5	1	1	1	1	0.25	0.64
H28	0.25	1	0.67	0.33	0.33	1	1	1	0.5	0.5	1	0.5	0.5	1	0.375	0.6
H29	1	0.75	0.67	0.33	0.33	0.5	0.5	1	0.5	0.25	0.33	0.5	0.5	0.5	0.5	0.5
H30	0.5	1	0.33	0.67	0.33	0.5	0.5	0.5	0.5	0.5	1	1	0.5	1	0.5	0.58
H31	0.5	0.75	0.33	0.33	1	1	0.5	1	0.5	0.75	1	1	0.5	1	0.375	0.65
H32	1	0.75	0.67	1	0.67	0.5	0.5	1	0.5	0.75	0.33	0.5	0.5	1	0.375	0.63
H33	0.5	0.5	0.67	0.33	1	1	1	0.5	0.5	0.75	1	1	1	1	0.5	0.7
H34	1	0.75	1	1	0.33	0.5	0.5	1	0.5	0.75	1	0.5	0.5	1	0.5	0.68
H35	0.5	0.75	0.67	0.67	0.33	1	0.5	1	0.5	0.5	1	1	0.5	1	0.5	0.65
H36	0.75	1	0.33	0.67	0.33	1	0.5	0.5	0.5	0.75	1	1	0.5	0.5	0.5	0.61
H37	0.75	0.75	0.33	0.33	0.67	1	0.5	0.5	0.5	0.75	1	1	0.5	1	0.5	0.63
H38	1	1	1	1	0.33	0.5	0.5	0.5	0.5	0.75	0.33	0.5	0.5	1	0.5	0.61
H39	0.75	1	0.67	1	0.33	1	0.5	1	0.5	0.75	1	1	0.5	0.5	0.625	0.7
H40	0.75	0.5	1	1	0.33	1	0.5	0.5	1	0.75	1	0.5	0.5	1	0.875	0.7
H41	0.75	0.75	0.67	1	0.67	0.5	1	0.5	1	0.75	1	1	0.5	1	0.875	0.77
H42	0.75	0.75	0.67	1	0.67	1	0.5	0.5	1	0.75	1	1	0.5	1	0.875	0.77
H43	0.5	0.5	0.67	0.33	0.33	1	1	0.5	1	0.25	1	0.5	1	1	1	0.64
H44	0.5	1	0.33	0.33	0.33	1	0.5	1	0.5	0.75	0.67	1	0.5	0.5	1	0.61
H45	1	0.5	0.33	1	0.33	0.5	0.5	0.5	0.5	0.75	0.33	1	0.5	1	1	0.6
H46	0.5	0.5	0.67	0.33	0.33	0.5	0.5	1	0.5	0.75	1	1	0.5	1	1	0.62
H47	0.5	0.75	0.67	0.33	0.33	1	0.5	1	0.5	0.25	1	0.5	0.5	1	1	0.6
H48	1	0.5	0.33	1	0.33	1	0.5	1	0.5	0.75	1	0.5	0.5	1	1	0.67
H49	0.5	0.75	0.67	0.33	0.33	1	0.5	1	0.5	0.25	1	0.5	0.5	0.5	1	0.57
H50	0.5	1	0.67	0.33	0.67	1	0.5	0.5	0.5	0.5	1	1	0.5	1	1	0.67

Table 7 (continued)

Building ID	R1	R2	R3	R4	R5	R6	R7	R8	R9	R10	R11	R12	R13	R14	R15	R
H51	1	0.25	0.67	1	0.33	1	0.5	0.5	0.5	0.75	1	1	0.5	1	0.875	0.66
H52	1	0.25	0.67	1	0.33	1	0.5	0.5	0.5	0.75	1	1	0.5	1	0.625	0.65
H53	0.5	1	0.67	0.33	0.33	1	0.5	0.5	0.5	0.5	1	0.5	0.5	1	0.875	0.6
H54	1	0.5	0.33	1	1	0.5	0.5	0.5	0.5	0.75	1	0.5	1	1	0.875	0.68
H55	1	0.75	1	1	0.67	0.5	0.5	0.5	0.5	0.75	1	1	0.5	0.5	0.625	0.69
H56	0.75	0.75	0.67	0.67	1	0.5	1	0.5	0.5	0.75	0.67	1	0.5	1	0.875	0.72
H57	1	0.75	1	1	1	1	1	0.5	1	0.75	1	1	0.5	1	1	0.88
H58	0.75	0.75	0.67	1	0.33	0.5	0.5	0.5	0.5	0.75	1	1	0.5	1	1	0.68
H59	0.75	0.75	1	1	0.67	1	1	0.5	0.5	0.25	1	0.5	0.5	1	1	0.71
H60	0.5	0.5	1	1	0.33	1	0.5	0.5	0.5	0.75	1	1	0.5	1	1	0.7
H61	0.5	0.5	0.67	0.33	1	0.5	1	0.5	0.5	0.75	1	1	0.5	1	0.75	0.66
H62	0.75	1	0.67	0.33	0.33	1	0.5	0.5	0.5	0.25	0.33	0.5	0.5	0.5	0.625	0.51
H63	0.5	1	0.33	0.33	0.33	1	1	1	0.5	0.25	1	0.5	0.5	1	0.625	0.59

R1, year of construction; R2, no. of floors; R3, roof material and design; R4, structural typology; R5, surrounding wall; R6, distance between windows and doors equal to or greater than 1 m; R7, distance between two houses equal to or greater than 1 m; R8, presence of windows and openings in the building facing the slope; R9, surrounding ambience; R10, state of maintenance; R11, type of construction; R12, retrofitted building; R13, presence of warning signs; R14, horizontal configuration; R15, position of building from the slope



Resistance Class
■ Low ($R < 0.5$)
■ Moderate ($0.5 < R < 0.9$)
 Landslide 2019

Fig. 5 Buildings falling under different resistance classes

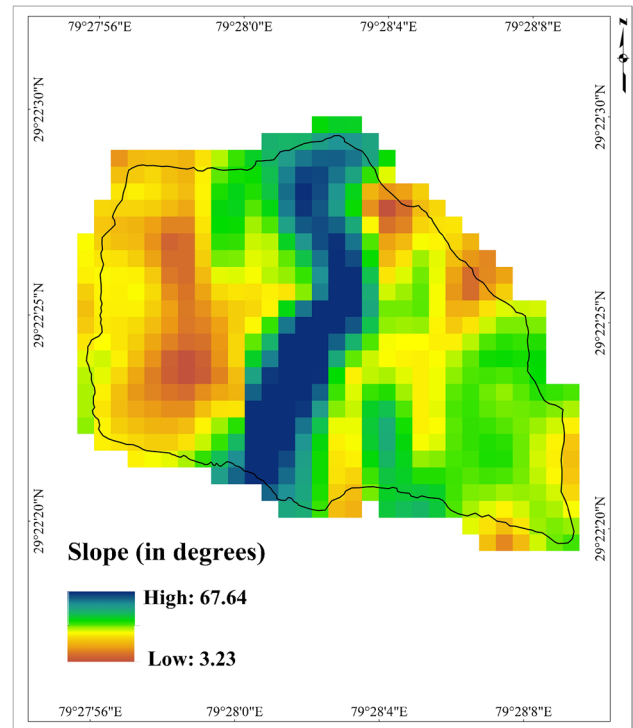


Fig. 6 Slope map of Balia Nala landslide

Table 8 Calculated site-specific vulnerability of buildings

Building ID	Physical vulnerability (PV)	Proximity of building to landslide	Site-specific vulnerability (SSV)	SSV class
H1	1	0–20 m	1	Class III
H2	1	0–20 m	1	Class III
H3	1	0–20 m	1	Class III
H4	1	0–20 m	1	Class III
H5	1	0–20 m	1	Class III
H6	1	21–40 m	0.95	Class III
H7	1	21–40 m	0.95	Class III
H8	1	21–40 m	0.95	Class III
H9	1	0–20 m	1	Class III
H10	1	21–40 m	0.95	Class III
H11	1	21–40 m	0.95	Class III
H12	1	21–40 m	0.95	Class III
H13	1	21–40 m	0.95	Class III
H14	1	21–40 m	0.95	Class III
H15	1	21–40 m	0.95	Class III
H16	1	21–40 m	0.95	Class III
H17	1	21–40 m	0.95	Class III
H18	1	21–40 m	0.95	Class III
H19	1	21–40 m	0.95	Class III
H20	1	21–40 m	0.95	Class III
H21	1	21–40 m	1	Class III
H22	1	0–20 m	1	Class III
H23	1	0–20 m	1	Class III
H24	1	0–20 m	1	Class III
H25	1	21–40 m	0.95	Class III
H26	1	21–40 m	0.95	Class III
H27	1	21–40 m	0.95	Class III
H28	1	21–40 m	0.95	Class III
H29	1	41–60 m	0.9	Class II
H30	1	41–60 m	0.9	Class II
H31	1	41–60 m	0.9	Class II
H32	1	41–60 m	0.9	Class II
H33	1	61–80 m	0.85	Class II
H34	1	61–80 m	0.85	Class II
H35	1	41–60 m	0.9	Class II
H36	1	41–60 m	0.9	Class II
H37	1	41–60 m	0.9	Class II
H38	1	41–60 m	0.9	Class II
H39	1	61–80 m	0.85	Class II
H40	1	101–120 m	0.75	Class II
H41	1	101–120 m	0.75	Class II
H42	1	121–140 m	0.7	Class II
H43	1	101–120 m	0.75	Class II
H44	1	81–100 m	0.8	Class II
H45	1	81–100 m	0.8	Class II
H46	1	81–100 m	0.8	Class II
H47	1	81–100 m	0.8	Class II
H48	1	81–100 m	0.8	Class II

Table 8 (continued)

Building ID	Physical vulnerability (PV)	Proximity of building to landslide	Site-specific vulnerability (SSV)	SSV class
H49	1	81–100 m	0.8	Class II
H50	1	81–100 m	0.8	Class II
H51	1	61–80 m	0.85	Class II
H52	1	61–80 m	0.85	Class II
H53	1	101–120 m	0.75	Class II
H54	1	101–120 m	0.75	Class II
H55	1	61–80 m	0.85	Class II
H56	1	81–100 m	0.8	Class II
H57	1	141–160 m	0.65	Class II
H58	1	81–100 m	0.8	Class II
H59	1	101–120 m	0.75	Class II
H60	1	81–100 m	0.8	Class II
H61	1	61–80 m	0.85	Class II
H62	1	41–60 m	0.9	Class II
H63	1	61–80 m	0.85	Class II

Class II ($0.5 < SSV \leq 0.9$) and class III ($0.9 < SSV \leq 1$)

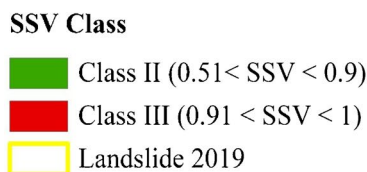
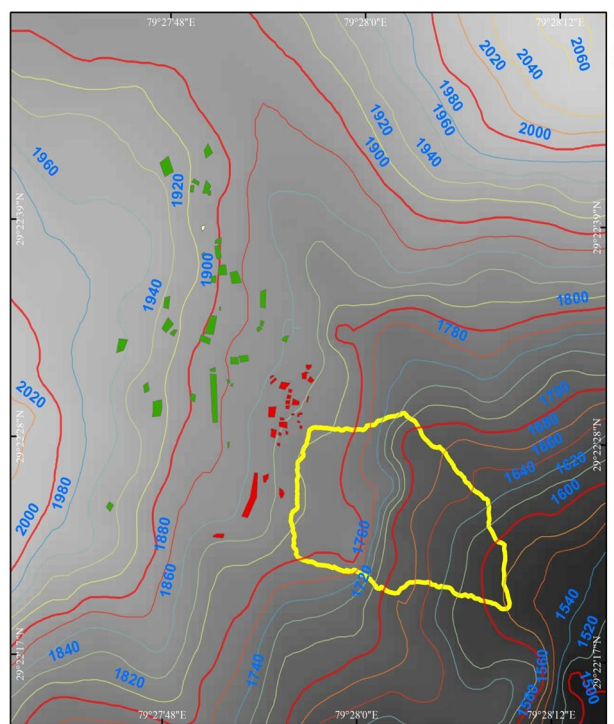


Fig. 7 Buildings falling under different SSV classes

Fig. 8 **a** Field photograph of building ID: H24 (R : 0.48, SSV class: III); **b** field photograph of building ID: H37 (R : 0.63, SSV class: II); **c, d** field photograph of building ID: H43 (R : 0.64, SSV class: II)



of '1' for all the surveyed households, owing to very high landslide intensity. The value is indicative of the fact that in a probable landslide scenario, the buildings would get totally damaged, which practically is not realistic, as proximity to the landslide also plays a major role. Hence, the site-specific physical vulnerability was calculated, and it was found that 56% of the surveyed households fall under class II ($0.5 < SSV \leq 0.9$; moderate to severe damage) and 44% fall under class III ($0.9 < SSV \leq 1$; very severe to complete damage). While in the first case, functionality of the buildings would get compromised and would demand retrofitting at a high cost, whereas in the other, complete damage would occur, offering no scope for retrofitting. This outcome is an issue of great concern as none of the buildings falls under class I ($SSV \leq 0.5$; low damage). Interestingly, it is noticed that some of the moderately resistant buildings (building IDs H4–7, H9, H11, H13–17, H19–23, H25–28) fall under SSV class III, after considering the 'proximity' to the landslide zone. Overall, the results show that the buildings in the study area are highly vulnerable. Any triggering factor like a severe earthquake or heavy rainfall scenario would pose a risk to the lives and property. Hence, the concerned authorities need to pre-plan their relocation and take all the possible remedial measures.

The haphazard and illegal constructions in the study area also need serious attention. Specific guidelines on building design and construction in earthquake-prone regions are available in India; however, this is not the case with respect to the landslide-prone region. This research opens a new avenue to frame or revise proper guidelines on building

constructions and design, specifically concerning landslides in the hilly terrain. It also highlights the need to take disaster risk reduction measures to reduce the landslide intensity and increase the resistance of buildings. Also, it recommends constantly monitoring the growing illegal constructions in the area with the objective to reduce disaster risk and promote sustainable development.

Conclusion

Balia Nala landslide has become an issue of great concern these days amongst the residents and researchers due to its frequent reactivation and burgeoning haphazard construction over its slope. These mandates characterize the Balia Nala landslide and quantify the physical vulnerability of the buildings. Thus, the indicator-based approach used by Singh et al. (2019a, b) with the aid of GIS has been adopted in the study area to assess the site-specific physical vulnerability of the buildings. The vulnerability of the 63 household samples was computed using 15 different indicators. Many other empirical relationships were employed to estimate the intensity of the landslide, resistance of the buildings, physical vulnerability (PV), and site-specific vulnerability (SSV). The landslide intensity obtained in the study is very high (1). About 89% of buildings fall under the category of moderate resistance ($0.5 < R \leq 0.9$), whereas 11% fall under the low resistance ($R \leq 0.5$) category. The physical vulnerability of all the buildings obtained is the same, i.e. 1. Since this is not

realistic, proximity to the landslide is taken as a criterion. About 56% of the buildings fall in class II ($0.5 < SSV \leq 0.9$), which is moderate to severe destruction and 44% of the buildings fall under class III ($0.9 < SSV \leq 1$) that is prone to extreme destruction. Hence, this quantification of physical vulnerability of the buildings and the characterization of the Balia Nala landslide will entail for improved understanding of the landslide and can help in suggesting necessary remedial measures for the buildings to support mitigation and decision-making and has the potential to customize the guidelines for building constructions for landslide in the region. The study can benefit concerned authorities like State Disaster Management Authority (SDMA), Uttarakhand; Irrigation Department, Nainital; and town planners for taking necessary and efficient Disaster Risk Reduction (DRR) measures which can contribute in reducing the landslide intensity, increasing the resistance of the buildings, and prioritizing relocation of the vulnerable households in case of any major landslide disaster in the future.

Acknowledgements The authors would like to acknowledge the concerned authorities of the Irrigation Department, Nainital, Uttarakhand, for providing useful information and data on the Balia Nala landslide. The authors are very much thankful to Dr Seabrat Das, Sr. Geologist, Geological Survey of India (GSI), Dehradun, for providing the landslide details and to Mr Manaruchi Mohapatra, an alumnus of Indian Institute of Remote Sensing, ISRO, Dehradun, for his valuable inputs in the initial phase of data collection.

Data availability The data used is clearly presented in the manuscript.

Code availability NA.

Declarations

Ethics approval NA.

Conflict of interest The authors declare no competing interests.

References

- Adger WN (2006) Vulnerability. *Global Environ Chang* 16(3):268–281. <https://doi.org/10.1016/j.gloenvcha.2006.02.006>
- Aleotti P, Chowdhury R (1999) Landslide hazard assessment: summary review and new perspectives. *Bull Eng Geol Environ* 58:21–44. <https://doi.org/10.1007/s100640050066>
- Anbazhagan S, Ramesh V (2014) Landslide hazard zonation mapping in Ghat road section of Kolli Hills, India. *J Mt Sci* 11(5):1308–1325. <https://doi.org/10.1007/s11629-012-2618-9>
- Bera S, Guru B, Oommen T (2020) Indicator-based approach for assigning physical vulnerability of the houses to landslide hazard in the Himalayan region of India. *Int J Disast Risk Re* 50:101891. <https://doi.org/10.1016/j.ijdr.2020.101891>
- Bhandari RK (1987) Slope instability in the fragile Himalaya and strategy for development. *Indian Geotech J* 17(1):1–78
- BIS (2016) National building code of India. Volume 1. In: National building code of India (Vol. 80, p. 1 v. (various pagings))
- Bründl M, Romang HE, Bischof N, Rheinberger CM (2009) The risk concept and its application in natural hazard risk management in Switzerland. *Nat Hazards Earth Syst Sci* 9(3):801–813. <https://doi.org/10.5194/nhess-9-801-2009>
- Cardinali M, Reichenbach P, Guzzetti F, Ardizzone F, Antonini G, Gali M, Cacciano M, Castellani M, Salvati P (2002) A geomorphological approach to the estimation of landslide hazards and risks in Umbria, Central Italy. *Nat Hazards Earth Syst Sci* 2:57–72. <https://doi.org/10.5194/nhess-2-57-2002>
- Chen Q, Chen L, Gui L, Yin K, Shrestha DP, Du J, Cao X (2020) Assessment of the physical vulnerability of buildings affected by slow-moving landslides. *Nat Hazards Earth Syst Sci* 20:2547–2565. <https://doi.org/10.5194/nhess-20-2547-2020>
- Cieslik K, Shakya P, Uprety M, Dewulf A, Russell C, Clark J, Dhital MR, Dhakal A (2019) Building resilience to chronic landslide hazard through citizen science. *Front Earth Sci* 7:278. <https://doi.org/10.3389/feart.2019.00278>
- Cruden DM, Varnes DJ (1996) Landslide types and processes. In: Landslides: investigation and mitigation. Transportation research board, special report 247:36–75
- Dai FC, Lee CF, Ngai YY (2002) Landslide risk assessment and management: an overview. *Eng Geol* 64(1):65–87. [https://doi.org/10.1016/S0013-7952\(01\)00093-X](https://doi.org/10.1016/S0013-7952(01)00093-X)
- Del Soldato M, Di Martire D, Bianchini S, Tomas R, De Vita P, Ramondini M, Casagli N, Calcaterra D (2019) Assessment of landslide-induced damage to structures: the Agnone landslide case study (southern Italy). *Bull Eng Geol Environ* 78:2387–2408. <https://doi.org/10.1007/s10064-018-1303-9>
- Dey J, Sakhre S, Vijay R, Bherwani H, Kumar R (2020) Geospatial assessment of urban sprawl and landslide susceptibility around the Nainital lake, Uttarakhand, India. *Environ Dev Sustain* 23:3543–3561. <https://doi.org/10.1007/s10668-020-00731-z>
- Di Traglia F, Bartolini S, Artesi E, Nolesini T, Ciampalini A, Lagomarsino D, Marti J, Casagli N (2018) Susceptibility of intrusion-related landslides at volcanic islands: the Stromboli case study. *Landslides* 15:21–29. <https://doi.org/10.1007/s10346-017-0866-z>
- Dikshit A, Sarkar R, Pradhan B, Acharya S, Alamri AM (2020) Spatial landslide risk assessment at Phuentsholing, Bhutan. *Geosci J* 10(4):131. <https://doi.org/10.3390/geosciences10040131>
- Du J, Yin K, Wang Y, Wu Y, Chai B (2016) Quantitative vulnerability evaluation of individual landslide: application to the Zhaoshuling landslide, Three Gorges Reservoir, China. In: Proceeding of 12th international symposium on landslides, Vol. 2, June 12th–19th, Napoli, Italy
- Du J (2012) Risk assessment of individual landslide. PhD thesis, China University of Geosciences
- Erener A, Düzgün HSB (2011) A GIS and RS-based quantitative vulnerability assessment for rainfall triggered landslides. In: 34th international symposium on remote sensing of environment, The GEOSS era: towards operational environmental monitoring. Sydney, Australia. <http://www.isprs.org/proceedings/2011/ISRSE-34/>
- Ettinger S, Mounaud L, Magill C, Yao-Lafourcade A-F, Thouret J-C, Manville V, Negulescu C, Zuccaro G, Gregorio DD, Nardone S, Uchuchoque JAL, Arguedas A, Macedo L, Llerena NM (2016) Building vulnerability to hydro-geomorphic hazards: estimating damage probability from qualitative vulnerability assessment using logistic regression. *J Hydrol* 541:563–581. <https://doi.org/10.1016/j.jhydrol.2015.04.017>
- Fuchs S, Heiss K, Hübl J (2007) Towards an empirical vulnerability function for use in debris flow risk assessment. *Nat Hazards Earth Syst Sci* 7:495–506. <https://doi.org/10.5194/nhess-7-495-2007>
- Glade T, Crozier M (2005) A review of scale dependency in landslide hazard and risk analysis. In: Glade T et al (eds) *Landslide hazard*

- and risk, John Wiley and Sons, England, pp 75–138. <https://doi.org/10.1002/9780470012659.ch3>
- Guillard-Gonçalves C, Zêzere JL, Pereira S, Garcia AC (2016) Assessment of physical vulnerability of buildings and analysis of landslide risk at the municipal scale: application to the Loures municipality, Portugal. *Nat Hazards Earth Syst Sci* 16:311–331. <https://doi.org/10.5194/nhess-16-311-2016>
- Guo Z, Chen L, Yin K, Shrestha DP, Zhang L (2020) Quantitative risk assessment of slow-moving landslides from the viewpoint of decision-making: a case study of the Three Gorges Reservoir in China. *Eng Geol* 273:105667. <https://doi.org/10.1016/j.enggeo.2020.105667>
- Gupta V, Bhasin RK, Kaynia AM (2016) Landslide hazard in the Nainital township, Kumaun Himalaya, India: the case of September 2014 Balia Nala landslide. *Nat Hazards* 80(2):863–877. <https://doi.org/10.1007/s11069-015-2002-5>
- Guzzetti F, Carrara A, Cardinali M, Reichenbach P (1999) Landslide hazard evaluation: a review of current techniques and their application in a multi-scale study, Central Italy. *Geomorphology* 31:181–216. [https://doi.org/10.1016/S0169-555X\(99\)00078-1](https://doi.org/10.1016/S0169-555X(99)00078-1)
- Guzzetti F, Ardizzone F, Cardinali M, Rossi M, Valigi D (2009) Landslide volumes and landslide mobilization rates in Umbria, central Italy. *Earth Planet Sc Lett* 279(3–4):222–229. <https://doi.org/10.1016/j.epsl.2009.01.005>
- Hukku BM, Srivastava AK, Jaitli GN (1974) Evolution of lakes around Nainital and the problem of hillside instability. *Himal Geol* 4:516–531
- Hungri O (1997) Some methods of landslide intensity mapping. In: Cruden and Fell (eds) *Landslide risk assessment, Proceedings of the international workshop on landslide risk assessment*, Honolulu, 19–21 February, Rotterdam: Balkema. pp 215–226
- IS 14458 (1997) Retaining wall for hill area - guidelines, part 2 design of retaining/breast wall
- IS 14804 (2000) Siting, design and selection of materials for residential buildings in hilly areas—guidelines In: Bureau of Indian Standards, New Delhi, India.
- Jaboyedoff M, Carrea D, Derron M-H, Oppikofer T, Penna IM, Rudaz B (2020) A review of methods used to estimate initial landslide failure surface depths and volumes. *Eng Geol* 267:105478. <https://doi.org/10.1016/j.enggeo.2020.105478>
- Jakob M, Stein D, Ulmi M (2012) Vulnerability of buildings to debris flow impact. *Nat Hazards* 60:241–261. <https://doi.org/10.1007/s11069-011-0007-2>
- Jones S, Kasthurba AK, Bhagyanathan A, Binoy BV (2021) Impact of anthropogenic activities on landslide occurrences in southwest India: an investigation using spatial models. *J Earth Syst Sci* 130:70. <https://doi.org/10.1007/s12040-021-01566-6>
- Joshi GC, Ghildiyal S, Rautela P (2019) Seismic vulnerability of life-line buildings in Himalayan province of Uttarakhand in India. *Int J Disast Risk Re* 37:101168. <https://doi.org/10.1016/j.ijdr.2019.101168>
- Kang H, Kim Y (2016) The physical vulnerability of different types of building structure to debris flow events. *Nat Hazards* 80:1475–1493. <https://doi.org/10.1007/s11069-015-2032-z>
- Kappes MS, Pappathoma-Köhle M, Keiler M (2012) Assessing physical vulnerability for multi-hazards using an indicator-based methodology. *Appl Geogr* 32(2):577–590. <https://doi.org/10.1016/j.apgeog.2011.07.002>
- Khanduri S, Mitigation D, Centre M (2019) Natural hazards in the township of Nainital, Uttarakhand in India. *Int J Eng Appl Sci Technol* 3(12):42–49
- Kotlia BS, Joshi LM, Dumka RK, Kumar K (2009) Vulnerability of the Balia Nala landslide at Nainital: preliminary GPs analysis. In: Sah BL (ed) *Natural resource conservation in Uttarakhand*. Ankit Publication, Haldwani, pp 136–150
- Kumar M, Rana S, Dutt P et al (2017) Slope stability analysis of Balia Nala landslide, Kumaun Lesser Himalaya, Nainital, Uttarakhand, India. *J Rock Mech Geotech Eng* 9(1):150–158. <https://doi.org/10.1016/j.jrmge.2016.05.009>
- Kuri M, Arora MK, Sharma ML (2018) Slope stability analysis in Nainital town using PS and QPS InSAR technique. *International geoscience and remote sensing symposium (IGARSS)*. pp 4443–4446. <https://doi.org/10.1109/IGARSS.2018.8517713>
- Lan HX, Zhou CH, Wang LJ, Zhang HY, Li RH (2004) Landslide hazard spatial analysis and prediction using GIS in the Xiaojiang watershed, Yunnan, China. *Eng Geol* 76:109–128. <https://doi.org/10.1016/j.enggeo.2004.06.009>
- Lee S, Min K (2001) Statistical analysis of landslide susceptibility at Yongin, Korea. *Environ Geol* 40:1095–1113. <https://doi.org/10.1007/s002540100310>
- Leone F, Asté JP, Velasquez E (1995) Contribution des constats d'endommagement au développement d'une méthodologie d'évaluation de la vulnérabilité appliquée aux phénomènes de mouvements de terrain. *Bull Assoc Géog Français* 4:350–371
- Li Z, Nadim F, Huang H, Uzielli M, Lacasse S (2010) Quantitative vulnerability estimation for scenario-based landslide hazards. *Landslides* 7(2):125–134. <https://doi.org/10.1007/s10346-009-0190-3>
- Malamud BD, Turcotte DL, Guzzetti F, Reichenbach P (2004) Landslides, earthquakes, and erosion. *Earth Planet Sc Lett* 229:45–59. <https://doi.org/10.1016/j.epsl.2004.10.018>
- Mavrouli O, Fotopoulou S, Ptilakis K, Zuccaro G, Corominas J, Santo A, Cacace F, De Gregorio D, Di Crescenzo G, Foerster E, Ulrich T (2014) Vulnerability assessment for reinforced concrete buildings exposed to landslides. *Bull Eng Geol Environ* 73:265–289. <https://doi.org/10.1007/s10064-014-0573-0>
- Medougall S (2014) Landslide runoff analysis – current practice and challenges. *Can Geotech J* 54(5):1–59
- Middlemiss CS (1898) Report on the Kailakhan landslip near Nainital of 17th August 1898. Government Press, Calcutta
- Nandi A, Shakoor A (2008) Application of logistic regression model for slope instability prediction in Cuyahoga River Watershed, Ohio, USA. *Georisk* 2(1):16–27. <https://doi.org/10.1080/17499510701842221>
- Ojeda-Moncayo J, Locat J, Couture R, Leroueil S (2004) The magnitude of landslides: an overview. In: Lacerda W, Ehrlich M, Fontoura AB, Sayao ASF (eds) *Landslides: evaluation and stabilization, Proceedings of the ninth international symposium on landslides*, June 28–July 2, Rio de Janeiro, Brazil. pp 379–384
- Pande RK, Pande N (2008) Nainital: a landslide town of Uttarakhand (India). *Disaster Prev Manag* 17(4):478–487. <https://doi.org/10.1108/09653560810901728>
- Papathoma-Köhle M, Neuhauser B, Ratzinger K, Wenzel H, Dominey-Howes D (2007) Elements at risk as a framework for assessing the vulnerability of communities to landslides. *Nat Hazards Earth Syst Sci* 7:765–779. <https://doi.org/10.5194/nhess-7-765-2007>
- Papathoma-köhle M, Gems B, Sturm M, Fuchs S (2017) Matrices, curves and indicators: a review of approaches to assess physical vulnerability to debris flows. *Earth-Sci Rev* 171:272–288. <https://doi.org/10.1016/j.earscirev.2017.06.007>
- Paul SK, Mahajan AK (1999) Malpa rockfall disaster, Kali Valley, Kumaun Himalaya. *Curr Sci India* 76(4):485–487
- Peng L, Xu S, Hou J, Peng J (2015) Quantitative risk analysis for landslides: the case of the Three Gorges area, China. *Landslides* 12:943–960. <https://doi.org/10.1007/s10346-014-0518-5>
- Quan Luna B, Blahut J, van Westen CJ et al (2011) The application of numerical debris flow modelling for the generation of physical vulnerability curves. *Nat Hazards Earth Syst Sci* 11(7):2047–2060
- Rautela P, Khanduri S, Bhaisora B, Pande KN, Ghildiyal S, Chanderkala C, Badoni S, Rawat A (2014) Implications of rapid land use/land cover changes upon the environment of the area around

- Nainital in Uttarakhand, India. *Asian Journal of Environment and Disaster Management (AJEDM) - Focusing on Pro-Active Risk Reduction in Asia* 06(01):69–79. <https://doi.org/10.3850/s1793924014000142>
- Rickenmann D (1999) Empirical relationships for debris flows. *Nat Hazards* 19:47–77. <https://doi.org/10.1023/A:1008064220727>
- Sah N, Kumar M, Upadhyay R, Dutt S (2018) Hill slope instability of Nainital City, Kumaun Lesser Himalaya, Uttarakhand, India. *J Rock Mech Geotech Eng* 10(2):280–289. <https://doi.org/10.1016/j.jrmge.2017.09.011>
- Saito H, Uchiyama S, Hayakawa YS, Obanawa H (2018) Landslides triggered by an earthquake and heavy rainfalls at Aso volcano, Japan, detected by UAS and SfM-MVS photogrammetry. *Prog Earth Planet Sci* 5:15. <https://doi.org/10.1186/s40645-018-0169-6>
- Sarkar S, Kanungo DP, Sharma S (2015) Landslide hazard assessment in the upper Alaknanda valley of Indian Himalayas. *Geomat Nat Haz and Risk* 6(4):308–325. <https://doi.org/10.1080/19475705.2013.847501>
- Satvati S, Alimohammadi H, Rowshanzamir M, Hejazi SM (2020) Bearing capacity of shallow footings reinforced with braid and geogrid adjacent to soil slope. *Int J Geosynth Ground Eng* 6:41. <https://doi.org/10.1007/s40891-020-00226-x>
- Sharma VK (2006) Zonation of landslide hazard for urban planning-case study of Nainital town, Kumaon Himalaya, India. IAEG, Paper Number 191, The Geological Society of London, 1–6
- Sidle RC, Ochiai H (2006) Landslides: processes, prediction, and landuse. American Geophysical Union, Washington, D.C. Water resources monograph no.18, pp 312
- Silva M, Pereira S (2014) Assessment of physical vulnerability and potential losses of buildings due to shallow slides. *Nat Hazards* 72:1029–1050. <https://doi.org/10.1007/s11069-014-1052-4>
- Singh A, Kanungo DP, Pal S (2018) A modified approach for semi-quantitative estimation of physical vulnerability of buildings exposed to different landslide intensity scenarios. *Georisk* 13(1):66–81. <https://doi.org/10.1080/17499518.2018.1501076>
- Singh A, Kanungo DP, Pal S (2019b) Physical vulnerability assessment of buildings exposed to landslides in India. *Nat Hazards* 96(2):753–790. <https://doi.org/10.1007/s11069-018-03568-y>
- Singh A, Pal S, Kanungo DP et al (2017) An overview of recent developments in landslide vulnerability assessment—presentation of a new conceptual framework. In: Mikoš M, Tiwari B, Yin Y, Sassa K (eds) *Advancing culture of living with landslides*, volume 2, advances in landslide science. pp 795–802. <https://doi.org/10.1007/978-3-319-53498-5>
- Singh A, Pal S, Kanungo DP (2019a) Site-specific vulnerability assessment of buildings exposed to rockfalls. In: Chattopadhyay J, Singh R, Prakash O (eds) *Renewable energy and its innovative technologies*. Springer, Singapore. https://doi.org/10.1007/978-981-13-2116-0_1
- Solari L, Bianchini S, Franceschini R, Barra A, Monserrat O, Thuegaz P, Bertolo D, Crosetto M, Catana F (2020) Satellite interferometric data for landslide intensity evaluation in mountainous regions. *Int J Appl Earth Obs* 87:102028. <https://doi.org/10.1016/j.jag.2019.102028>
- Thennavan E, Ganapathy GP, Chandra Sekaran SS, Rajawat AS (2016) Use of GIS in assessing building vulnerability for landslide hazard in the Nilgiris, Western Ghats, India. *Nat Hazards* 82(2):1031–1050. <https://doi.org/10.1007/s11069-016-2232-1>
- Turner BL, Kasperson RE, Matson PA, McCarthy JJ, Corell RW, Christensen L, Eckley N, Kasperson JX, Luers A, Martello ML, Polsky C, Pulsipher A, Schiller A (2003) A framework for vulnerability analysis in sustainability science. *Proc Natl Acad Sci USA* 100(14):8074–8079. <https://doi.org/10.1073/pnas.1231335100>
- Uzielli M, Nadim F, Lacasse S, Kaynia AM (2008) A conceptual framework for quantitative estimation of physical vulnerability to landslides. *Eng Geol* 102(3–4):251–256. <https://doi.org/10.1016/j.enggeo.2008.03.011>
- Uzielli M, Catani F, Tofani V, Casagli N (2015) Risk analysis for the Ancona landslide—II: estimation of risk to buildings. *Landslides* 12(1):83–100. <https://doi.org/10.1007/s10346-014-0477-x>
- Vaid R, Chattoraj SL, Mishra S et al (2019) Landslide hazard zonation mapping and debris flow modelling in Nainital, Uttarakhand. In: 2nd International Electronic Conference on Geosciences. <https://doi.org/10.3390/iecg2019-06221>
- Valdiya KS (1988) Geology and natural environment of Nainital hills, Kumaun Himalaya. Gyanodaya Prakashan, Nainital, India, pp 160
- Voogd H (1983) Multi criteria evaluation for urban and regional planning. Pion Limited, London, p 367
- Wakatsuki T, Tanaka Y, Matsukura Y (2005) Soil slips on weathering limited slopes underlain by coarse-grained granite or fine-grained gneiss near Seoul, Republic of Korea. *Catena* 60(2):181–203. <https://doi.org/10.1016/j.catena.2004.11.003>
- Yhokha A, Goswami PK, Changm C (2018) Application of persistent scatterer interferometry (PSI) in monitoring slope movements in Nainital, Uttarakhand Lesser Himalaya, India. *J Earth Syst Sci* 127(1):1–13. <https://doi.org/10.1007/s12040-017-0907-y>
- Zheng J, He H, Alimohammadi H (2021) Three-dimensional Wadell roundness for particle angularity characterization of granular soils. *Acta Geotech* 16:133–149. <https://doi.org/10.1007/s11440-020-01004-9>